

Original article

**Evaluation of glymphatic system activity with the diffusion MR
technique: Diffusion tensor image analysis along the
perivascular space (DTI-ALPS) in Alzheimer's disease cases.**

Toshiaki Taoka¹, Yoshitaka Masutani², Hisashi Kawai¹, Toshiki Nakane¹, Kiwamu
Matsuoka³, Fumihiko Yasuno³, Toshifumi Kishimoto³, Shinji Naganawa¹

1. Department of Radiology, Nagoya University,
65 Tsurumai-cho, Showa-ku, Nagoya, Aichi 466-8550, Japan
2. Dept. Biomedical Information Sciences, Graduate School of Information Sciences,
Hiroshima City University,
3-4-1, Ozuka-Higashi, Asa-Minami-Ku, Hiroshima, 731-3194, JAPAN
3. Department of Psychiatry, Nara Medical University,
840 Shijo-cho, Kashihara, Nara, 634-8522, Japan

Ethical statement

All applicable institutional and/or national guidelines for the care were followed.

Conflict of Interest:

The authors declare that they have no conflict of interest.

Corresponding Author

Toshiaki Taoka, M.D. Ph.D.
Department of Radiology, Nagoya University Hospital
65 Tsurumai-cho, Showa-ku, Nagoya, Aichi 466-8550, Japan
Tel: +81-52-744-2327, Fax: +81-52-744-2335
E-mail: ttaoka@med.nagoya-u.ac.jp

Word count: 2972 words

Original article

**Evaluation of glymphatic system activity with the diffusion MR technique:
Diffusion tensor image analysis along the perivascular space (DTI-ALPS)
in Alzheimer's disease cases.**

1
2
3
4
5
6
7
8
9
10
11
12
13
14
15
16
17
18
19
20
21
22
23
24
25
26
27
28
29
30
31
32
33
34
35
36
37
38
39
40
41
42
43
44
45
46
47
48
49
50
51
52
53
54
55
56
57
58
59
60
61
62
63
64
65

1
2
3
4
5
6 **Abstract**
7

8
9 **Purpose:** The activity of the glymphatic system is impaired in animal models of Alzheimer's disease
10
11 (AD). We evaluated the activity of the human glymphatic system in cases of AD with a diffusion-
12
13 based technique called Diffusion Tensor Image analysis Along the Perivascular Space (DTI-ALPS).
14
15

16
17 **Materials and methods:** Diffusion tensor images were acquired to calculate diffusivities in the x, y,
18
19 and z axes of the plane of the lateral ventricle body in 31 patients. We evaluated the diffusivity along
20
21 the perivascular spaces as well as projection fibers and association fibers separately, to acquire an
22
23 index for diffusivity along the perivascular space (ALPS-index) and correlated them with the mini
24
25 mental state examinations (MMSE) score.
26
27

28
29 **Results:** We found a significant negative correlation between diffusivity along the projection fibers
30
31 and association fibers. We also observed a significant positive correlation between diffusivity along
32
33 perivascular spaces shown as ALPS-index and the MMSE score, indicating lower water diffusivity
34
35 along perivascular space in relation to AD severity.
36
37

38
39 **Conclusion:** Activity of the glymphatic system may be evaluated with diffusion images. Lower
40
41 diffusivity along the perivascular space on DTI-APLS seems to reflect impairment of the glymphatic
42
43 system. This method may be useful for evaluating the activity of the glymphatic system.
44
45
46
47
48
49
50
51
52
53
54
55
56
57
58
59
60
61
62
63
64
65

1
2
3
4
5
6
7
8
9
10
11
12
13
14
15
16
17
18
19
20
21
22
23
24
25
26
27
28
29
30
31
32
33
34
35
36
37
38
39
40
41
42
43
44
45
46
47
48
49
50
51
52
53
54
55
56
57
58
59
60
61
62
63
64
65

Key words

Glymphatic system, Alzheimer's disease, MRI, Diffusion Tensor, Perivascular space

1
2
3
4
5 **Introduction**
6
7

8
9
10 The glymphatic system is a recently discovered waste drainage system in the brain that involves
11
12 movement of the cerebrospinal fluid (CSF) along the perivascular space. This system promotes
13
14 elimination of soluble proteins including amyloid- β ($A\beta$) and metabolites, and also facilitates the
15
16 distribution of glucose, lipids, amino acids, and neuromodulators (1-3). In this system, CSF and
17
18 interstitial fluid (ISF) interchange by influx of CSF along the loose fibrous matrix of perivascular
19
20 spaces (1). CSF influx from the subarachnoid space into the deep peri-arterial space is driven by
21
22 arterial pulsatile motion, slow motion of the vessels, respiratory motion, and CSF pressure.
23
24
25 Subsequently, CSF is transported into the brain parenchyma via aquaporin-P4 (AQP4) water channels
26
27
28 in astrocytic end-feet. CSF movement into the parenchyma drives convective ISF flux within the tissue
29
30 toward the peri-venous spaces surrounding the deep veins. ISF is then collected in the peri-venous
31
32 space. From the peri-venous space, the fluid drains out of the brain toward the cervical lymphatic
33
34 system (1,4,5). These activities of the glymphatic system have been studied by intrathecally
35
36 administered tracers in animal experiments (1). However, this method is invasive in humans due to
37
38 administration of tracers including gadolinium-based contrast medium (GBCM), and thus, any method
39
40
41 has not been established for evaluation of the glymphatic system in humans.
42
43
44
45
46
47
48
49
50
51
52
53
54
55
56
57
58

59 The purpose of the current study is to assess the feasibility of a non-invasive method **we coined**
60
61
62
63
64
65

1
2
3 “diffusion tensor image analysis along the perivascular space (DTI-ALPS)” for evaluating the activity
4
5
6 of the glymphatic system in human brain by using diffusion images. In this method, we evaluated the
7
8
9 motion of water molecule in the direction of the perivascular space by measuring diffusivity using the
10
11
12 diffusion tensor method (Figure 1). At the level of the lateral ventricle body, the medullary veins run
13
14
15 perpendicular to the ventricular wall (6), and the perivascular space runs in the same direction as the
16
17
18 medullary veins, which is the right-left direction (x-axis). On the plane of this area, projection fibers
19
20
21 run in the head-foot direction, mainly adjacent to the lateral ventricle, and superior longitudinal
22
23
24 fascicles (SLFs) representing association fibers in the current study run in the anterior-posterior
25
26
27 direction outside the projection fibers. Outside the SLFs, subcortical fibers run mainly in the right-left
28
29
30 direction in subcortical areas. Consequently, in this area, the perivascular space runs perpendicular to
31
32
33 the projection fibers and SLFs. This conformation of the perivascular space and major fibers in this
34
35
36 area allows nearly independent analysis of the diffusivity along the direction of the perivascular space
37
38
39 because major fiber tracts do not run parallel to the direction of the perivascular space. When there is
40
41
42 histological change along the right-left direction (x-axis), it will equally affect both projection and
43
44
45 association fibers. Thus, when such change is observed for both fiber bundles, it is probably safe to
46
47
48 state that at least part of this change comes from the pathology involving the perivascular space,
49
50
51 namely the glymphatic system.
52
53
54
55
56
57
58

59 Because the activity of the glymphatic system is reported to be impaired in AD according to
60
61
62
63
64
65

1
2
3 observations in animal experiments (2), we analyzed the different degrees of glymphatic system
4
5
6 activity by performing diffusion tensor studies of cases with Alzheimer's disease (AD), mild cognitive
7
8
9 impairment (MCI), and subjective cognitive impairment (SCI) with different degrees of severity.
10
11
12
13
14
15
16
17
18

19 **Materials and Methods**

20
21
22
23

24 We studied 31 patients (14 males and 17 females; age range 51 to 89 years old; mean 75 years; median
25
26 76 years), 16 with AD, nine with MCI, and six with SCI (Mini mental state examination (MMSE)
27
28 range: 12 to 30). We obtained permission from the institutional review board at the institute where the
29
30
31 imaging study was performed. Written informed consent for the imaging study was obtained from all
32
33
34 patients or their families after the nature of the procedures had been fully explained. Clinical diagnoses
35
36
37 of AD and MCI were based on the Diagnostic and Statistical Manual of Mental Disorders-IV criteria
38
39
40 and examination of the cognitive status, and diagnosis of SCI was made according to the proposed
41
42
43
44
45
46 Reisberg criteria for SCI (7). All subjects were right-handed. MMSE was performed for all subjects.
47
48
49
50

51 Diffusion imaging was acquired by using a 3.0-T clinical scanner (Magnetom Verio, Siemens AG,
52
53
54 Erlangen, Germany). DTI sets with $b = 0$ s/mm², $b = 1000$ s/mm², and $b = 2000$ s/mm² (Echo planer,
55
56
57 TR = 6600 ms, TE = 89 ms, MPG = 30 directions, FOV = 230 mm, matrix = 94 × 94, slice thickness
58
59
60

1
2
3 = 3 mm) were acquired simultaneously in addition to conventional morphology images.
4
5
6
7

8 Diffusion metric images were generated by using dTV.II.13k+ software (Dept. Biomedical
9
10 Information Sciences, Graduate School of Information Sciences, Hiroshima City University) (8). The
11
12 software creates computational images of the diffusion tensor including a color-coded fractional
13
14 anisotropy (FA) map and diffusivity map, and in addition, has the capability to calculate diffusivity in
15
16 the direction of the x-axis, y-axis, and z-axis on each image. Using this function, we performed
17
18 analyses with the DTI-ALPS method, which is used to evaluate the diffusivity along the direction of
19
20 the perivascular space compared with those of projection fibers and association fibers on a slice at the
21
22 level of the lateral ventricle body (Figure 1a). At that level, the direction of the perivascular space is
23
24 perpendicular to the ventricle wall and is thus mostly in the right-left direction (x-axis) on the axial
25
26 plane. The direction is also perpendicular to the direction of both the projection fibers (mostly in the
27
28 z-axis) and the association fibers (mostly in the y-axis) (Figure 1d). Thus, the diffusivity along the x-
29
30 axis at regions with projection/association fibers will at least partly represent the diffusivity along
31
32 the perivascular space. On a color color-coded FA map of the plane at the level of the lateral ventricle
33
34 body, we placed a 5-mm diameter spherical region of interest (ROI) in the area of the projection fibers
35
36 (blue on Figure 1c), the area of the association fibers (green on Figure 1c), and the area of the
37
38 subcortical fibers (red on Figure 1c) in the left hemisphere. For each area, we calculated the diffusivity
39
40 in the directions of the x-axis, y-axis, and z-axis and correlated them with the MMSE score of the
41
42
43
44
45
46
47
48
49
50
51
52
53
54
55
56
57
58
59
60
61
62
63
64
65

1
2
3 subjects to obtain a correlation coefficient and p-value. We obtained measurements only in the left
4
5
6 hemisphere in the current study, because all subjects were all right-handed and the SLF is thick enough
7
8
9 to place the ROI on the left side. We evaluated the statistical difference of the slope of the regression
10
11
12 curves with analysis of co-variance (ANCOVA).
13
14
15

16
17 In addition, we calculated an index which we will call as ALPS-index in order to evaluate the activity
18
19
20 of the glymphatic system in individual cases. This index is provided by the ratio of two sets of
21
22
23 diffusivity value which are perpendicular to dominant fibers in the tissue, that is the ratio of mean of
24
25
26 x-axis diffusivity in the area of projection fiber (D_{xproj}) and x-axis diffusivity in the area of
27
28
29 association fibers (D_{xassoc}) to the mean of y-axis diffusivity in the area of projection fiber (D_{yproj})
30
31
32 and z-axis diffusivity in the area of association fibers (D_{zassoc}) as follows.
33
34
35
36
37

$$38 \text{ ALPS index} = \frac{\text{mean}(D_{xproj}, D_{xassoc})}{\text{mean}(D_{yproj}, D_{zassoc})}$$

39
40
41
42

43 In the area of projection fibers, the dominant fibers runs in the direction of z-axis, and both x-axis and
44
45
46 y-axis are perpendicular to the dominant fibers. Similarly, in the area of association fibers, the
47
48
49 dominant fibers runs in the direction of y-axis, and both x-axis and z-axis are perpendicular to the
50
51
52 dominant fibers. The major difference for the water molecule behavior between x-axis diffusivity in
53
54
55 both area (D_{xproj} and D_{xassoc}) and the diffusivity which is perpendicular to them (D_{yproj} and
56
57
58 D_{zassoc}) would be the existence of the perivascular space. We also correlated this ALPS-index with
59
60
61
62
63
64
65

1
2
3 the MMSE score. We made the above mentioned analyses separately for the datasets with $b=1000$
4
5
6 s/mm^2 and $b=2000 s/mm^2$.
7
8
9

10 11 12 13 14 15 16 **Results**

17
18
19
20
21 The correlations between MMSE and diffusivities for the three directions (x, y, z) of the three areas
22
23 (projection, association, subcortical) are shown in Figure 2 with their correlation coefficients and
24
25 statistical significance (indicated as “*”). In the $b = 1000 s/mm^2$ datasets in the projection area, we
26
27 found a significant positive correlation ($r = 0.40$, $p = 0.026$) between the diffusivity along the
28
29 perivascular space (x-axis) and the MMSE scores, whereas the diffusivity along the projection fibers
30
31 (z-axis) showed a significant negative correlation ($r = -0.62$, $p = 0.00021$) with MMSE scores.
32
33
34
35
36
37
38
39
40 Diffusivity in the anterior-posterior direction (y-axis) did not show a correlation with MMSE scores
41
42
43 ($r = -0.24$, $p = 0.20$). Also in the $b = 1000 s/mm^2$ datasets in the association area, we found a significant
44
45
46 positive correlation ($r = 0.50$, $p = 0.0042$) between the diffusivity along the perivascular space (x-axis)
47
48
49 and the MMSE scores, whereas the diffusivity along the association fibers (y-axis) showed a
50
51
52 significant negative correlation ($r = -0.55$, $p = 0.0013$) with MMSE scores. Diffusivity in the head-
53
54
55 feet direction (z-axis) did not show a correlation with MMSE scores ($r = -0.10$, $p = 0.58$). No
56
57
58 statistically significant correlation was found between the diffusivity of the three directions and
59
60
61
62
63
64
65

1
2
3 MMSE scores in the subcortical area.
4
5
6

7
8 For the $b = 2000 \text{ s/mm}^2$ measurements, no statistically significant correlation was found between the
9
10 diffusivity and MMSE scores other than the diffusivity along the projection fibers (z-axis), which
11
12 showed a significant negative correlation ($r = -0.48$, $p = 0.0067$) with MMSE scores in the projection
13
14 area. With ANCOVA, statistically significant differences were found in the slope of the regression
15
16 line between the x-axis and z-axis in the projection area on $b = 1000 \text{ s/mm}^2$ images ($p < 0.001$) and
17
18 between the x-axis and y-axis in the association area on $b = 1000 \text{ s/mm}^2$ images ($p < 0.001$).
19
20
21
22
23
24
25
26

27
28 On the evaluation of ALPS-index, there were significant positive correlation ($r=0.46$, $p=0.0084$)
29
30 between the ALPS-index and the MMSE scores on the $b=1000\text{s/mm}^2$ datasets. While, on the
31
32 $b=2000\text{s/mm}^2$ measurements, there was not statistically significant correlation between the ALPS-
33
34 index and MMSE scores ($r=0.29$, $p=0.109$).
35
36
37
38
39
40
41
42
43
44
45
46

47 **Discussion**

48
49
50
51

52 The glymphatic system, which was first proposed in 2012 by Nedergaard et al., is the waste clearance
53
54 pathway system for CSF through the perivascular space and the interstitial space in the brain (1). A
55
56 recent report by Peng et al. indicated that glymphatic transport is suppressed in a mouse model of AD.
57
58
59
60

1
2
3 They reported that A β circulates through glymphatic pathways. Oligomerization may limit the
4
5
6 distribution of A β , and soluble A β oligomers, a more toxic form of A β , may also contribute to
7
8
9 glymphatic dysfunction. Long-term exposure to A β in the subarachnoid CSF may suppress glymphatic
10
11
12 transport prior to the presence of substantial A β deposits (9). Apolipoprotein E4 (apoE4) is a major
13
14
15 genetic risk factor for AD. However, how apoE4 influences AD onset and progression has yet to be
16
17
18 proven. A recent experimental report showed that the glymphatic fluid transport system contributes to
19
20
21 the delivery of choroid plexus/CSF-derived human apoE to neurons (10). Perivascular localization of
22
23
24 AQP4 facilitates the activity of the glymphatic system. Experimental mouse studies suggest that the
25
26
27 AQP4-dependent glymphatic pathway is an important clearance system for driving the removal of
28
29
30 soluble A β . In mice, A β is cleared along perivascular pathways, and A β clearance is reduced by 55-
31
32
33 65% in AQP4 knockout mice compared with wild-type mice (1). A recent report on postmortem
34
35
36 human brain tissue showed that perivascular AQP4 localization is significantly associated with AD
37
38
39 status independent of age (11).
40
41
42

43
44
45 Observation of the glymphatic system has been made with tracer studies in animal experiments (1-3).
46
47

48
49 Iliff et al. showed that CSF rapidly enters the brain along the cortical pial arteries following labeling
50
51
52 of CSF with fluorescent tracers injected into the CSF of the cisterna magna. The dynamics of the
53
54
55 glymphatic system were characterized for the first time in vivo using two-photon microscopy in mice
56
57
58 (1). In addition to fluorescence materials, intrathecal administration of GBCM was also used as a tracer
59
60

1
2
3 in later animal studies. An experimental rat study with whole-brain imaging following intrathecal
4
5
6 GBCM administration allowed identification of two key influx nodes at the pituitary and pineal gland
7
8
9 recesses (2). However, intrathecal administration of tracers in humans has not been performed except
10
11
12 for several well-designed studies (12,13) and an accident report (14). GBCM administration only into
13
14
15 CSF can cause T1 hyperintensity in the globus pallidus and dentate nucleus, strongly suggesting
16
17
18 involvement of the glymphatic system in the phenomenon of gadolinium deposition in the globus
19
20
21 pallidus or dentate nucleus (13). Naganawa et al. observed enhancement of the perivascular space and
22
23
24 CSF space on heavily T2-weighted FLAIR images 4 hours after intravenous injection of GBCM
25
26
27 (15,16); however, no method for tracing intravenously administered GBCM with MRI has been
28
29
30 established. In addition, even if a tracer method to evaluate the glymphatic system in living humans is
31
32
33 established, tracer studies of the glymphatic system require hours to follow the distribution of the
34
35
36 tracer within the brain, and monitoring the activity of the glymphatic system in real time is not possible.
37
38
39 Thus, monitoring methods other than tracer studies are needed to evaluate the glymphatic system. The
40
41
42 DTI-ALPS method used in the current study uses diffusion images, which can be acquired within
43
44
45 several minutes, and may have potential to monitor the status of the glymphatic system over time.
46
47
48

49
50
51 The DTI-ALPS method can be used to evaluate the diffusivity along the direction of the perivascular
52
53
54 space compared with the direction of projection fibers and association fibers on a slice at the level of
55
56
57 the lateral ventricle body. The medullary arteries and veins are the vessels of the brain parenchyma
58
59
60

1
2
3 and accompany the perivascular space, which is the major draining pathway of the glymphatic system.
4
5

6 It is still difficult to visualize fine medullary arteries on MR images, however, with use of 3-T scanners
7
8
9 and high resolution imaging protocols such as susceptibility-weighted imaging (SWI) that can be used
10
11
12 to visualize fine venous structures (17). Prior to the current evaluation, we examined SWIs and color
13
14
15 coded FA images of the normal brains and looked for the area in which conformation of the
16
17
18 perivascular space represented by medullary veins on SWI and the major white matter tracts are
19
20
21 perpendicular manner. We found that perivascular space runs in the right-left direction (x-axis),
22
23
24 projection fibers run in the head-foot (z-axis) direction, and association fibers run in the anterior-
25
26
27 posterior (y-axis) direction outside the projection fibers at the level of the lateral ventricle body.
28
29
30

31
32
33 Our results of the current study indicated a significant negative correlation between MMSE scores and
34
35
36 the diffusivity along the projection fibers and association fibers. This result can be explained by white
37
38
39 matter degeneration in the projection or association fibers due to AD or MCI as shown in a previous
40
41
42 report (18). In addition, an atlas-based analysis of DTI to survey 30 major cerebral white matter tracts
43
44
45 in AD cases indicated that association tracts have increases in mean, axial, and radial diffusivity, and
46
47
48 projection tracts have increases in axial and radial diffusivity, observations that are interpreted as
49
50
51 decreased tissue density in these tracts in AD cases (19). In contrast, our current study showed a
52
53
54 significant *positive* correlation between the diffusivity along the perivascular space and the MMSE
55
56
57 score, indicating impaired water diffusivity in the direction of the perivascular space in relation to AD
58
59
60

1
2
3 severity in areas with projection or association fiber dominance. Our results are consistent with the
4
5
6 impaired activity of the glymphatic system in AD suggested by experiments with rats (2). We made
7
8
9 this evaluation with two different b-values including $b= 1000 \text{ s/mm}^2$ as standard b-value and $b=2000$
10
11
12 s/mm^2 as higher b-value. In order to assure better signal to noise ratio, we did not selected very high
13
14
15 b-value such as $b=3000 \text{ s/mm}^2$. The observation above such as positive correlation between ALPS-
16
17
18 index and MMSE was more obvious in the measurement with $b = 1000 \text{ s/mm}^2$ than that with $b = 2000$
19
20
21 s/mm^2 . Since influence from water molecule with higher motivity become dominant when the b-value
22
23
24 is lower, higher diffusivity or motivity of water molecule within the perivascular space could have a
25
26
27 larger influence with a rather lower b-value ($b= 1000 \text{ s/mm}^2$) measurement. Another possible reason
28
29
30 for the difference between $b= 1000 \text{ s/mm}^2$ and $b=2000 \text{ s/mm}^2$ is the higher signal to noise ratio which
31
32
33 is acquired in the measurement with $b= 1000 \text{ s/mm}^2$.
34
35
36
37
38
39

40 We calculated ALPS-index in order to evaluate the activity of the glymphatic system in individual
41
42 cases. On this index, we hypothesized that the ratio of x-axis diffusivity in projection fibers and
43
44 association fibers area (D_{xproj} and D_{xassoc}) to the diffusivity which is perpendicular to them (D_{yproj}
45
46 and D_{zassoc}) would express the influence of the water diffusion along perivascular space which will
47
48
49 reflect activity of the glymphatic system in the individual cases. When the ratio is closed to 1, it means
50
51
52 that the influence of the water diffusion along the perivascular space is the minimum, and larger ratio
53
54
55 will represent larger water diffusivity along the perivascular space. In our result, there were significant
56
57
58
59
60

1
2
3 positive correlation between the ALPS-index and the MMSE scores on the $b=1000s/mm^2$ datasets.
4
5

6 This result would indicate that the ALPS-index can be used for evaluating the activity of the
7
8
9
10 glymphatic system in the individual cases. The result also indicated that the cases with lower MMSE
11
12
13 score only distribute in lower ALPS-index. It may indicate that the cases with severe AD has impaired
14
15
16 glymphatic system almost without exception. On the other hand, ALPS-index has wide variety in the
17
18
19 cases with high MMSE score. There may be other unknown factors which impairs glymphatic system
20
21
22 in some cases with mild AD or MCI, SCI cases.
23
24
25

26
27 Our current study has several limitations. At this moment, our software can calculate the diffusivity
28
29
30 only on x, y and z axis, which are obtained as the components of diffusion tensor; D_x , D_y , and D_z .
31
32

33
34 Therefore, the area outside the lateral ventricle along the plane of the lateral ventricle body is the only
35
36
37 place where we can independently evaluate the diffusivity along the direction of the perivascular space.
38
39

40 In areas in which the perivascular space does not run in the direction of the x, y, or z axes or areas in
41
42
43 which the perivascular space and the direction of the predominant fiber tract are parallel, isolated
44
45
46 evaluation of the diffusivity along the perivascular space is impossible. Another limitation is that the
47
48
49 ROI was placed manually, which may be a subjective factor of our measurement. However, we tried
50
51
52 to place ROI as objectively as possible. The small number of subjects and the fact that the study was
53
54
55 performed at a single institute are other limitations. In addition, we did not take any other physiological
56
57
58 status into account, including perfusion or pulsatile motion of the brain. However, we performed
59
60

1
2
3 diffusion imaging with $b = 1000 \text{ s/mm}^2$ and $b = 1000 \text{ s/mm}^2$, because this rather high motion gradient
4
5
6 is expected to cancel out the rather macroscopic physiological status.
7
8
9

10
11 In conclusion, our results using the DTI-ALPS method demonstrated a significant positive correlation
12
13 between the diffusivity along the perivascular space and the MMSE score, indicating impaired water
14
15 diffusivity related to AD, MCI, or SCI severity. Thus, lower diffusivity along the perivascular space
16
17 or lower ALPS-index seems to reflect impairment of the glymphatic system. The DTI-APLS method
18
19 can be used for evaluating the activity of the glymphatic system, and the ALPS-index may be applied
20
21
22
23
24
25
26
27 for evaluating conditions that affect the activity of the glymphatic system of the individual cases.
28
29
30
31
32
33
34
35
36
37
38
39
40
41
42
43
44
45
46
47
48
49
50
51
52
53
54
55
56
57
58
59
60
61
62
63
64
65

1
2
3 **References**
4
5

- 6 1. Iliff JJ, Wang M, Liao Y, Plogg BA, Peng W, Gundersen GA, et al. A paravascular
7 pathway facilitates CSF flow through the brain parenchyma and the clearance of
8
9 interstitial solutes, including amyloid beta. *Sci Transl Med* 2012;4(147):147ra11.
10
11
12
13
14
15
16 2. Iliff JJ, Lee H, Yu M, Feng T, Logan J, Nedergaard M, et al. Brain-wide pathway for
17
18 waste clearance captured by contrast-enhanced MRI. *J Clin Invest* 2013;123(3):1299-
19
20
21
22 309.
23
24
25 3. Jessen NA, Munk AS, Lundgaard I, Nedergaard M. The Glymphatic System: A
26
27
28 Beginner's Guide. *Neurochem Res* 2015;40(12):2583-99.
29
30
31
32 4. Johnston M, Zakharov A, Papaiconomou C, Salmasi G, Armstrong D. Evidence of
33
34
35 connections between cerebrospinal fluid and nasal lymphatic vessels in humans, non-
36
37
38 human primates and other mammalian species. *Cerebrospinal Fluid Res* 2004;1(1):2.
39
40
41 5. Murtha LA, Yang Q, Parsons MW, Levi CR, Beard DJ, Spratt NJ, et al. Cerebrospinal
42
43
44 fluid is drained primarily via the spinal canal and olfactory route in young and aged
45
46
47 spontaneously hypertensive rats. *Fluids Barriers CNS* 2014;11:12.
48
49
50
51 6. Okudera T, Huang YP, Fukusumi A, Nakamura Y, Hatazawa J, Uemura K. Micro-
52
53
54 angiographical studies of the medullary venous system of the cerebral hemisphere.
55
56
57 *Neuropathology* 1999;19(1):93-111.
58
59
60
61
62
63
64
65

- 1
2
3 7. Reisberg B, Prichep L, Mosconi L, John ER, Glodzik-Sobanska L, Boksay I, et al. The
4
5
6 pre-mild cognitive impairment, subjective cognitive impairment stage of Alzheimer's
7
8
9 disease. *Alzheimers Dement* 2008;4(1 Suppl 1):S98-S108.
10
- 11
12 8. Masutani Y, Aoki S, Abe O, Hayashi N, Otomo K. MR diffusion tensor imaging: recent
13
14
15
16 advance and new techniques for diffusion tensor visualization. *Eur J Radiol*
17
18
19 2003;46(1):53-66.
20
- 21
22 9. Peng W, Achariyar TM, Li B, Liao Y, Mestre H, Hitomi E, et al. Suppression of
23
24
25
26 glymphatic fluid transport in a mouse model of Alzheimer's disease. *Neurobiol Dis*
27
28
29 2016;93:215-25.
30
- 31
32 10. Achariyar TM, Li B, Peng W, Verghese PB, Shi Y, McConnell E, et al. Glymphatic
33
34
35
36 distribution of CSF-derived apoE into brain is isoform specific and suppressed during
37
38
39 sleep deprivation. *Mol Neurodegener* 2016;11(1):74.
40
- 41
42 11. Zeppenfeld DM, Simon M, Haswell JD, D'Abreo D, Murchison C, Quinn JF, et al.
43
44
45
46 Association of Perivascular Localization of Aquaporin-4 With Cognition and
47
48
49 Alzheimer Disease in Aging Brains. *JAMA Neurol* 2016;74(1):91-99.
50
- 51
52 12. Tali ET, Ercan N, Krumina G, Rudwan M, Mironov A, Zeng QY, et al. Intrathecal
53
54
55
56 gadolinium (gadopentetate dimeglumine) enhanced magnetic resonance
57
58
59 myelography and cisternography: results of a multicenter study. *Invest Radiol*
60
61
62
63
64
65

- 1
2
3 2002;37(3):152-9.
4
5
6
7 13. Oner AY, Barutcu B, Aykol S, Tali ET. Intrathecal Contrast-Enhanced Magnetic
8
9 Resonance Imaging-Related Brain Signal Changes: Residual Gadolinium Deposition?
10
11 Invest Radiol 2016.
12
13
14
15
16 14. Samardzic D, Thamburaj K. Magnetic resonance characteristics and susceptibility
17
18 weighted imaging of the brain in gadolinium encephalopathy. J Neuroimaging
19
20
21
22 2015;25(1):136-9.
23
24
25
26 15. Naganawa S, Nakane T, Kawai H, Taoka T. Gd-based Contrast Enhancement of the
27
28 Perivascular Spaces in the Basal Ganglia. Magn Reson Med Sci 2016;16(1):61-65.
29
30
31
32 16. Naganawa S, Suzuki K, Yamazaki M, Sakurai Y. Serial scans in healthy volunteers
33
34 following intravenous administration of gadoteridol: time course of contrast
35
36 enhancement in various cranial fluid spaces. Magn Reson Med Sci 2014;13(1):7-13.
37
38
39
40
41 17. Taoka T, Fukusumi A, Miyasaka T, Kawai H, Nakane T, Kichikawa K, et al. Structure
42
43 of the Medullary Veins of the Cerebral Hemisphere and Related Disorders.
44
45 Radiographics 2017;37(1):281-97.
46
47
48
49
50
51 18. Fellgiebel A, Yakushev I. Diffusion tensor imaging of the hippocampus in MCI and
52
53 early Alzheimer's disease. J Alzheimers Dis 2011;26 Suppl 3:257-62.
54
55
56
57 19. Huang H, Fan X, Weiner M, Martin-Cook K, Xiao G, Davis J, et al. Distinctive
58
59
60
61
62
63
64
65

1
2
3
4
5
6
7
8
9
10
11
12
13
14
15
16
17
18
19
20
21
22
23
24
25
26
27
28
29
30
31
32
33
34
35
36
37
38
39
40
41
42
43
44
45
46
47
48
49
50
51
52
53
54
55
56
57
58
59
60
61
62
63
64
65

disruption patterns of white matter tracts in Alzheimer's disease with full diffusion
tensor characterization. Neurobiol Aging 2012;33(9):2029-45.

1
2
3 **Figure legends**
4
5
6
7

8 **Figure 1: Concept for the diffusion tensor image analysis along the perivascular space (DTI-**
9 **ALPS) method**
10

11
12
13
14
15
16 a: Roentgenogram of an injected coronal brain slice showing parenchymal vessels that run horizontally
17
18 on the slice (white box) at the level of the lateral ventricle body. Reproduced with permission from
19
20 reference (6).
21
22

23
24
25
26
27 b: Axial SWI on the slice at the level of the lateral ventricle body indicates that parenchymal vessels
28
29 run laterally (x-axis).
30
31

32
33
34
35 c: Superimposed color display of DTI on SWI (b) indicating the distribution of projection fibers (z-
36
37 axis: blue), association fibers (y-axis: green), and the subcortical fibers (x-axis: red). Three ROIs are
38
39 placed in the area with projection fibers (projection area), association fibers (association area) and
40
41 subcortical fibers (subcortical area) to measure diffusivities of the three direction (x, y, z).
42
43
44
45
46
47

48
49 d: Schematic indicating the relationship between the direction of the perivascular space (gray cylinder)
50
51 and the directions of the fibers. Note that the direction of the perivascular space is perpendicular to
52
53 both projection and association fibers.
54
55
56
57
58
59
60

1
2
3
4
5
6
7
8 **Figure 2: Correlation between directional diffusivity and MMSE scores**
9

10
11
12 Correlation between MMSE and diffusivities for the three directions of the three areas (projection: a,
13 d, association: b, e, subcortical: c, f) with the $b = 1000$ s/mm² datasets (a, b, c) and the $b = 2000$ s/mm²
14
15
16 datasets (d, e, f). Diffusivity of the x-axis is plotted as red, y-axis as green, and z-axis as blue.
17
18
19
20
21
22 Regression lines are also shown in the same colors with the plots, accompanied by values for the
23
24
25 correlation coefficient. Statistically significant correlations are shown as “*”.
26
27

28
29
30 On the $b = 1000$ s/mm² datasets, in the projection area (a), we found a significant positive correlation
31
32
33 between the diffusivity along the perivascular space (x-axis) and the MMSE scores. In the association
34
35
36 area (b), we found a significant positive correlation between the diffusivity along the perivascular
37
38
39 space (x-axis) and the MMSE scores. On the other hand, there were significant negative correlation
40
41
42 between the diffusivity along the projection fiber (z-axis) in the projection area and the MMSE scores.
43

44
45
46 There were also significant negative correlation between the association fiber (y-axis) in the association
47
48
49 area and the MMSE scores. These negative correlation may be explained by white matter degeneration
50
51
52 in the projection or association fibers due to AD or MCI. On the $b = 2000$ s/mm² measurements, we
53
54
55 found no statistically significant correlations between the diffusivity and MMSE scores other than the
56
57
58 diffusivity along the projection fibers (z-axis), which showed a significant negative correlation with
59
60

1
2
3 MMSE scores in the projection area . Statistically significant differences ($p < 0.001$) for the regression
4
5
6 line were identified with ANCOVA between the x-axis (red) and z-axis (blue) in the projection area
7
8
9 on $b = 1000 \text{ s/mm}^2$ images (a) and between the x-axis (red) and y-axis (green) in the association area
10
11
12 on $b = 1000 \text{ s/mm}^2$ images (b).
13
14
15
16
17
18
19
20
21

22 **Figure 3 Correlation between ALPS-index and MMSE.**

23
24
25
26

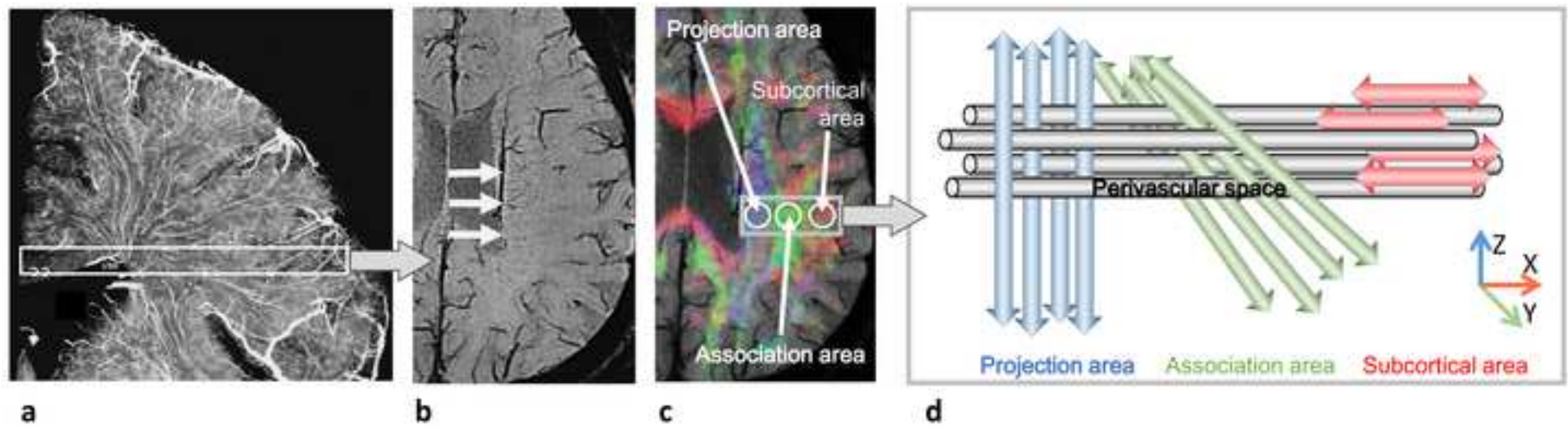
27 Correlation between MMSE and ALPS-index which is given by following ratio are shown (a:

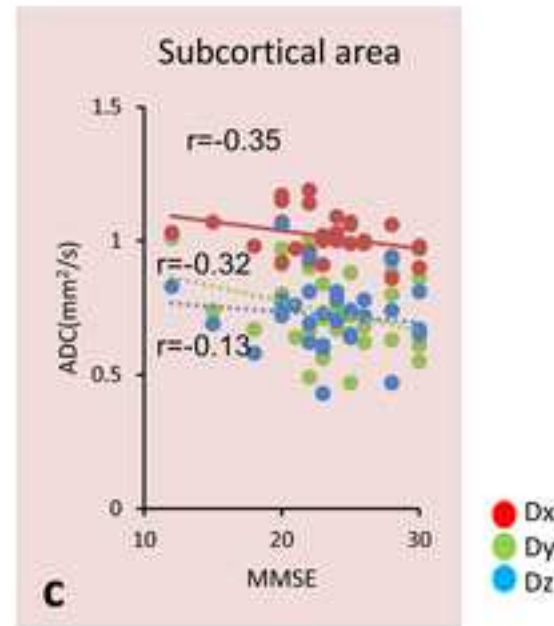
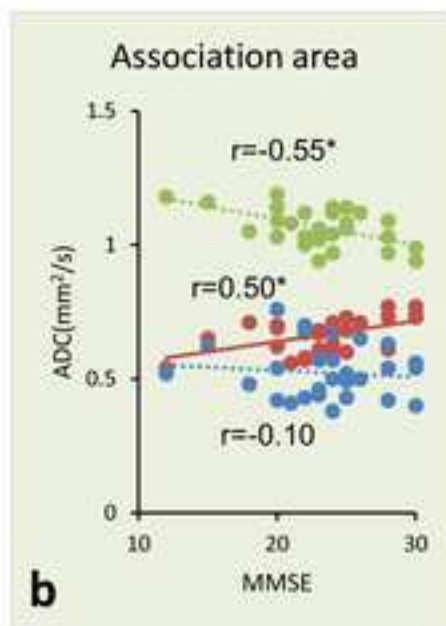
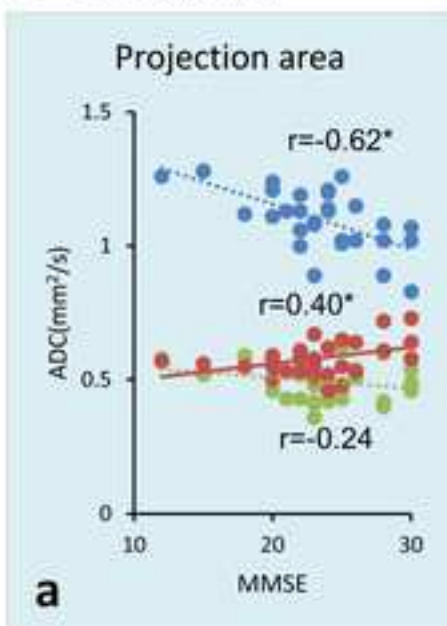
28
29
30 $b=1000\text{s/mm}^2$, b: $b=2000\text{s/mm}^2$).
31
32
33
34

$$35 \text{ALPS index} = \frac{\text{mean} (D_{xproj}, D_{xassoc})}{\text{mean} (D_{yproj}, D_{zassoc})}$$

36
37
38
39

40 There were significant positive correlation ($r=0.46$, $p=0.0084$) between the ALPS-index and the
41
42
43 MMSE scores on the $b=1000\text{s/mm}^2$ datasets (a). While, on the $b=2000\text{s/mm}^2$ measurements (b), there
44
45
46 was no statistically significant correlation between the ALPS-index to MMSE scores ($r=0.29$,
47
48
49 $p=0.109$). Note that the cases with lower MMSE score shows lower ALPS-index closed to 1, while
50
51
52
53 ALPS index has wide variety in the cases with high MMSE score.
54
55
56
57
58
59
60
61
62
63
64
65



$b=1000s/mm^2$  $b=2000s/mm^2$ 